New Journal of Physics
The open access journal at the forefront of physics

Deutsche Physikalische Gesellschaft DPG IOP Institute of Physics

PAPER • OPEN ACCESS

# Routes to control Cooper minimum in high order harmonics generated in argon gas

To cite this article: G S Boltaev *et al* 2020 *New J. Phys.* **22** 083031

New Journal of Physics
The open access journal at the forefront of physics

Deutsche Physikalische Gesellschaft DPG
IOP Institute of Physics

Published in partnership with: Deutsche Physikalische Gesellschaft and the Institute of Physics

OPEN ACCESS

RECEIVED
7 April 2020

REVISED
18 June 2020

ACCEPTED FOR PUBLICATION
1 July 2020

PUBLISHED
12 August 2020



PAPER

# Routes to control Cooper minimum in high order harmonics generated in argon gas

G S Boltaev[1,2], R A Ganeev[1,3], N A Abbasi[1], M Iqbal[1], V V Kim[1], H Al-Harmi[1], X M Tong[4] and A S Alnaser[1,5]

[1] Department of Physics, American University of Sharjah, PO Box 26666, Sharjah, United Arab Emirates
[2] Tashkent Institute of Irrigation and Agricultural Mechanization Engineers, Tashkent 100000, Uzbekistan
[3] Faculty of Physics, Voronezh State University, Voronezh 394006, Russia
[4] Center for Computational Sciences, University of Tsukuba, 1-1-1 Tennodai, Tsukuba, Ibaraki 305-8573, Japan
[5] Author to whom any correspondence should be addressed.

**E-mail:** gboltaev@aus.edu and aalnaser@aus.edu

**Keywords:** Cooper minimum, high harmonics generation, strong field ionization

## Abstract

We present a systematic study on the control of Cooper minimum (CM) in the high-order harmonics spectra generated during the interaction of Ar gas with ultrashort near-infrared laser pulses. Tailoring the width and depth of CM in argon is demonstrated by changing the gas jet position with respect to the focal plane of focusing lens and by defocusing-assisted phase-matching. We further analyze the influence of single- and two-color laser pump schemes on the appearance of CM. The application of two orthogonally-polarized fields of fundamental radiation and its second harmonic, which is also used to generate controllable yields of odd and even harmonics, led to diminishing the CM in the harmonic spectra. Our experimental findings are supported by theoretical calculations that solve the time-dependent Schrödinger equation in the microscopic domain, and take into account the phase matching in the macroscopic domain.

## 1. Introduction

High-order harmonic generation (HHG) in gases is a well-developed technique for generating coherent extreme ultraviolet (XUV) radiation [1]. Among the motivations for investigating HHG is to probe and characterize atomic and molecular structures using high-order harmonic emission on attosecond timescale [2]. The observation of distinct local minimum in the high-order harmonic emission from noble gas targets can be considered a finger print of these targets [3–5]. This so called Cooper minimum (CM) is also present in the XUV photoionization of noble gases [6]. The appearance of the minimum in the harmonics distribution from single-atom HHG spectrum of Ar has been attributed to radiative recombination of an electron to atomic ion, which is the inverse process of photoionization where the cross section has a minimum. Analyzing the characteristics of CM in the HHG spectra has been also extended to molecules [7].

HHG can be well explained by the three-step model proposed by Corkum [8], where the radiative recombination step is more precisely described by quantitative rescattering (QRS) theory [9], which relates the minimum of HHG to the minimum of the photoionization cross section of the parent atomic target [10]. Apart from describing HHG in the microscopic domain, which can be calculated using the strong field approximation (SFA), QRS theory, or by directly solving the time-dependent Schrödinger equation, one has to consider also the phase matching effects in the macroscopic domain. For example, macroscopic propagation effects are different for HHGs from Bessel beams compared to Gaussian beams [11], although the atomic HHG with both beams at the microscopic level are the same. This also shows the complexity of the HHG at the macroscopic scale.

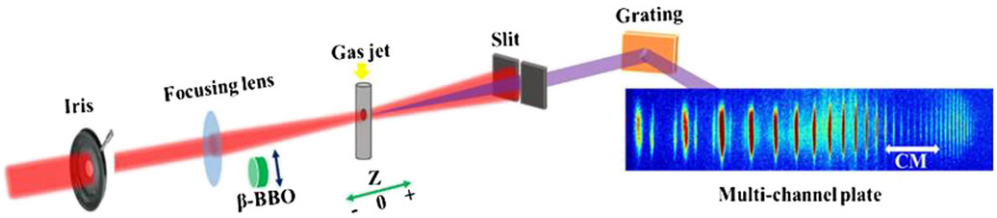


**Figure 1.** High-repetition rate near-infrared source for generation of coherent XUV pulses. We used the 600 $\mu$J pulses from Yb fiber laser at central wavelength of 1030 nm, 36 fs pulse duration, and 50 kHz repetition rate. Inset shows the raw image of high-order harmonics spectrum generated in argon with indication of Cooper minimum (CM) and distinction of harmonic divergences.

The interest in the spectral minima of HHG is related to the photoionization studies of atoms or molecules from different atomic or molecular orbitals. Based on QRS theory, CM occurs when the photoionization cross-section goes through a minimum. In the case of Ar, the driving field of the laser pulse removes an electron from the 3*p* orbital and therefore recombination occurs back to the 3*p* state. The Cooper minimum in argon is very prominent at around 49 eV and has been extensively studied [12–15]. The first study of CM in HHG was described in reference [12].

In this work, we analyze methods to control the dynamics of CM under different experimental conditions and explain this process by studying atomic HHG at the microscopic level as well as phase matching effects at the macroscopic level. We consider the influence of single- and two-color fields from near-infrared laser pulses on the behavior of CM by analyzing HHG spectra in Ar gas. We investigate HHG in gases (atoms and molecules) with very similar ionization potential using single-color, and two-color orthogonally-polarized laser fields at high pulse repetition rate (50 kHz). The variation in the width and the depth of CM in the XUV harmonic spectra generated in Ar gas was explored by changing the position of gas jet with respect to the focal plane and by defocusing-assisted phase mismatch, in addition to applying two orthogonally-polarized laser pulses. The interaction of atoms with two orthogonally-polarized fields has been an effective tool for enhancing the harmonic yield and for simultaneous generation of odd and even orders of harmonics in laser-produced plasmas [16]. Furthermore, we perform a theoretical study that solves the time-dependent Schrödinger equation to obtain atomic HHG in microscopic level and consider the phase matching effects at the macroscopic level. Our theoretical results are in good agreement with the experimental ones in reproducing the position of the observed minimum and in describing the disappearance of CM when two electromagnetic fields interact with Ar atoms.

## 2. Experimental arrangements

The experimental setup is shown in figure 1. The high repetition rate fiber laser system provides driving laser pulse with 36 fs duration and 0.6 mJ energy at a central wavelength of 1030 nm. The beam was focused using a focusing lens with $f = 400$ mm into a gas jet installed on translating stage inside the vacuum chamber.

The focusing conditions provided spot size of 50 $\mu$m radius. The corresponding confocal parameter of the focused diffraction-limited beam was $\sim$15.2 mm. The estimated intensity of the driving 1030 nm beam was $\sim 2 \times 10^{14}$ W cm$^{-2}$.

We used an iris aperture to control the beam diameter and energy of the focused pulses. The energy of the driving pulse was changed from 370 $\mu$J up to 600 $\mu$J after going through the irises of 8 and 20 mm diameters, respectively. The intensity was varied by changing the diameters of the aperture. This allowed us controlling the intensity as well as the defocusing-assisted phase matching conditions. For the second harmonic (SH) generation, a type-I beta-barium borate (BBO) crystal was placed inside the vacuum chamber on the path of the focused driving beam to avoid extra group velocity dispersion when going through the window of the chamber and the focusing lens, as well as to exclude the beam walk-off. SH conversion efficiency of $\sim$3% was obtained by using 0.1 mm thick BBO crystal. The raw image of HHG spectrum generated in argon at the maximal intensity of laser pulses is shown in figure 1. CM is clearly distinguished in the HHG spectrum by the difference in the divergence and brightness of harmonics at its location. Gas jet with a circular nozzle of 1.5 mm diameter was used as a target. The inner diameter of the gas nozzle (1 mm) was considered to be the effective length of the nonlinear media. The pressure of gases was maintained at $\sim 10^4$ Pa (70 Torr) inside the vacuum chamber at the area of interaction with the femtosecond pulses. The HHG spectrum was analyzed using XUV spectrometer.

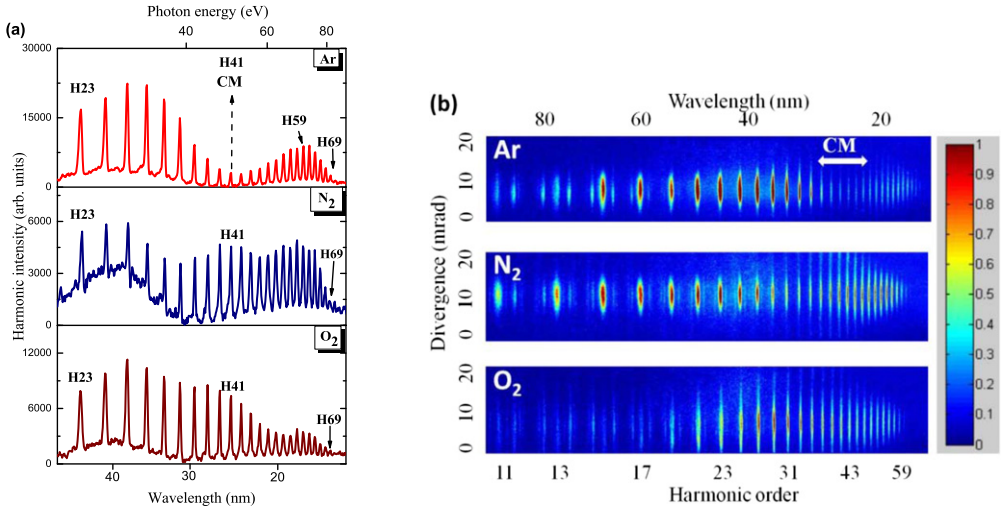


**Figure 2.** Harmonic spectra generated in noble and molecular gases of similar ionization potential. (a) Spectra of harmonics produced in argon (upper panel, first ionization potential 15.759 eV), nitrogen (middle panel, ionization potential 15.58 eV for molecular HOMO orbital $2\sigma_g$), and oxygen (bottom panel, ionization potential 12.07 eV for molecular HOMO orbital $2\pi_g$) using 600 $\mu$J pulses. The dashed black arrow shows the position of CM in the spectrum of HHG in Ar gas. (b) Raw images of harmonics [argon (upper panel), nitrogen (middle panel), and oxygen (bottom panel)]. The CM is seen at around of 24 nm in the case of argon gas. White arrow shows the position of CM. The saturated images of harmonics are presented for better viewing of harmonic orders and divergence variations in the cases of three gases.

## 3. Experimental results

Figure 2 shows the comparative spectral and spatial distributions of the high-order harmonics (HH) generated in Ar, $N_2$ and $O_2$ at very similar experimental conditions. Due to the closeness of the ionization potentials in Ar and $N_2$ gases we observed similar harmonic cutoffs for 1030 nm, 36 fs pulses. However, a characteristic CM centered at ~25 nm is observed only in the case of Ar [figures 2(a) and (b), upper panels]. In the case of $O_2$ with ionization potential of 12.07 eV, the extension of harmonic cutoff is attributed to the ionization suppression, which has been demonstrated in [17]. In the case of $O_2$, due to the dependence of the cutoff energy on the wavelength ($E_{\text{cutoff}} \sim I \times \lambda^2$), it was possible to produce 80 eV photons at an intensity less than $2.1 \times 10^{14}$ W cm$^{-2}$ using 1030 nm pulses. An extended plateau, as well as relatively strong 11th ($\lambda = 93.6$ nm) and 13th ($\lambda = 79.2$ nm) harmonics, were observed in the case of nitrogen gas [figure 2(b), middle panel], when compared to the other two gases (Ar and $O_2$) at the same experimental conditions. In the case of $O_2$, we observed gradual decrease of harmonic yield starting from 25th order [figures 2(a) and (b), bottom panels].

The intensities of different harmonics as well as the width and depth of CM were analyzed at different experimental conditions, particularly by varying the intensity and spatial conditions of the driving 1030 nm pulses and by using two-color laser pump, as shown in figure 3. In these experiments we changed the driving beam sizes using an iris with variable diameter. We also moved the gas jet at different positions with respect to the focal plane of focusing lens. The disappearance of CM by changing the phase-matching conditions based on the defocusing-assisted phase mismatch of the driving pulses in Ar is shown in figure 3(a) [$E_\omega = 470$ $\mu$J, at the 12 mm beam diameter after the iris]. We also analyzed the dependence of CM width on the energy of the driving laser pulses. The panels in figure 3(a) show the dependence of harmonic cutoff energy on the energy of the driving femtosecond pulses. The increase of the energy of laser pulses led to increase in the cutoff energy. During these experiments, harmonics up to the 69th order [$\lambda =$ 14.9 nm, upper panel of figure 3(a)] were observed. In the case of two-color pump scheme, no CM was observed with the variation of the beam diameter [figure 3(b)], but, we observed strong odd and even harmonics yields as a function of the total energy of the driving and SH pulses ($E_\omega + E_{2\omega}$).

Figure 4 shows the variations of HHG spectra at different positions of the gas jet with respect to the focal plane of the focusing lens. The focal plane was determined by measuring the minimal size of focused beam. We measured the beam profile by using CCD camera-based beam profiler (Thorlabs) at the low energy of driving pulses. We found the minimal beam spot size by scanning the beam profiler along the propagation direction of the driving pulses. We analyzed the variations of the width and depth of CM by changing the position of the Ar gas jet. In the upper panel ($z = +3$ mm) of figure 4(a), HHG spectrum of Ar is shown for the position when the gas jet was placed after the focal plane of the focusing lens. In this

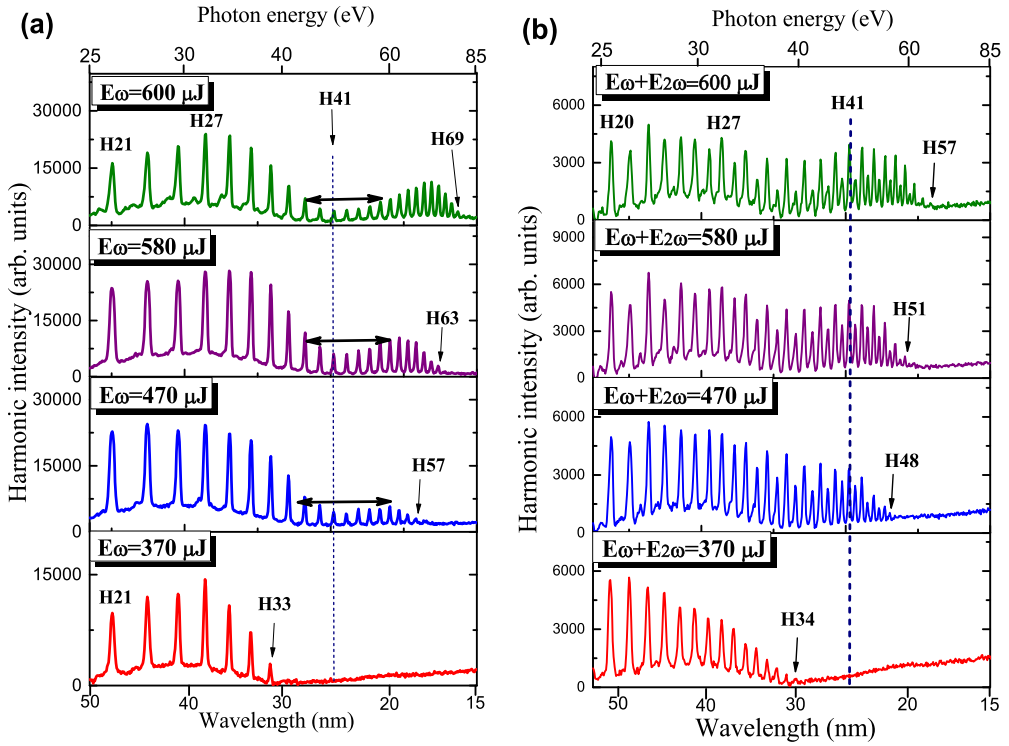


**Figure 3.** Spectra of harmonics generated in Ar at different experimental conditions. (a) Modification of cutoff energy by changing the diameter of the iris placed in front of the focusing spherical lens in the case of single-color pump (1030 nm). The dashed black line shows the position of CM at the photon energy ~49 eV (H41). The solid arrows show the width of CM. (b) Same dependences are presented in the case of orthogonally polarized two-color pump (1030 nm + 515 nm) of argon, which show the absence of CM. Dashed black line in this figure shows the position of CM in the case of single-color pump.

case one can see wide and deep CM in the harmonic spectrum. By moving the gas jet towards the focal plane (middle panel $z = 0$), the CM became larger. Meanwhile, when the gas jet was placed before laser focus (bottom panel of figure 4(a), $z = -3$ mm), the width of CM again became narrower. The confocal parameter of focused radiation was equal to ~15.2 mm. Thus even at these ratios between the confocal parameter and variations of jet position the small deviation from focal position led to almost complete disappearance of CM. Notice that in the case of molecular gas ($O_2$, figure 4(b)), no significant change in the harmonic spectra at these three positions of gas jet was observed. Since the IR intensities at $z = +3$ mm and $-3$ mm are approximately the same as far as the focus size is concerned, the difference of the HHG in the upper and lower panels of figure 4(b) originates from the difference in the phase matching conditions. The contribution of the short trajectories of free electron for harmonic generation is optimal at the conditions when gas target is located before the focal plane of focusing lens. We also observed the high divergence of HHG in the cutoff range for the position when the gas jet is located behind the focal plane.

The appearance of Cooper minimum in the spectra of high-order harmonics is associated with the photoionization of argon in XUV range. The CM width in HHG spectrum is conventionally defined by the variation of the harmonics intensity in the vicinity of the CM position. In our case, this parameter was determined by measuring the intensity of weakest harmonic in the CM and defining the lower- and higher-harmonic orders intensities of which were twice stronger with regard to the CM harmonic (H41). In other words, the width of this minimum is defined by full width half minimum of the valley, by analogy with the full width half maximum of the intensity distribution in the cases of determination of the beam sizes, spectra, etc. The width of CM did not change significantly with the decrease of the energy of the driving pulse in the case of single-color pump (figure 3(a)) and was maximal at the position of Ar gas jet at the focal plane (figure 4(a)).

Our theoretical estimates (see section 4) show that the CM width can be slightly broadened by the strong IR laser field due to the ac stark shift. However, this range of laser intensities was not reached during these experiments. Based on experimental results one can estimate the intensity of driving pulses ($\sim 2 \times 10^{14}$ W cm$^{-2}$) at which CM width remains almost unchanged.

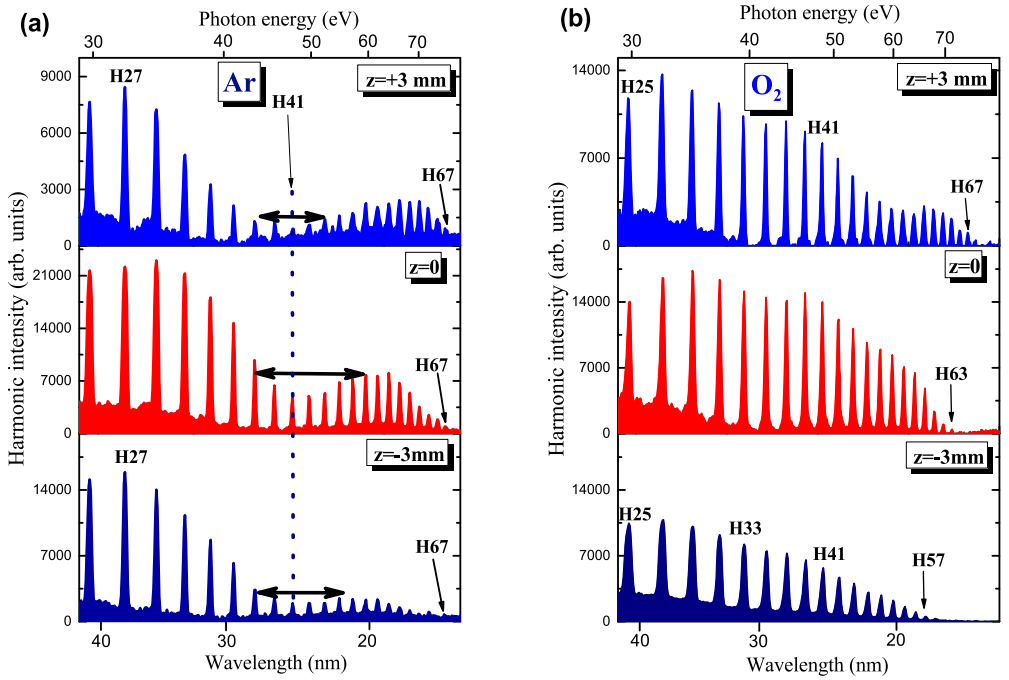


**Figure 4.** Dependences of harmonic spectra on the position of the gas jet with regard to the focal plane of focusing lens in the case of single-color pump. (a) Variation of the width and depth of CM in the HHG spectrum of Ar using 1030 nm laser pulses. Vertical dashed black line shows the position of CM. Horizontal arrows show the width of CM. The largest value of CM width was observed at the position of gas jet in the focal plane ($z = 0$ mm). (b) Variation of maximal harmonic order by changing the position of $O_2$ gas jet. One can see the absence of CM in the case of oxygen. The Ar and $O_2$ gas jets were installed at different positions with respect to the laser focus on $z$-axis of the propagation of laser beam. Upper panels correspond to $z = +3$ mm (i.e. behind the focal plane); middle panels correspond to $z = 0$ (i.e. focal plane); bottom panels correspond to $z = -3$ mm (i.e. in front of focal plane) positions of gas jet.

## 4. Theoretical results

To understand the underlying mechanisms of the experimental observations, we also studied theoretically HHG of Ar atoms by solving the time-dependent Schrödinger equation (TDSE) under the single active electron approximation with a model potential [18]. Since orthogonally-polarized laser fields were used in the experiment, we solved the full three-dimensional TDSE [17, 19]. To consider the focal volume effect and phase matching in the propagation, we solved the TDSE thousand times for different IR intensities and different ratios of the two-color laser fields. Since CM may be washed out after the phase matching process as shown in figure 4(a), we present the atomic HHG without the focal volume averaging and phase matching first to study the dynamics of the CM in HHG at the atomic level. The convergence of the simulation was checked by comparing the results from length and acceleration forms and we only present the HHG from the acceleration form. Figure 5 shows the HHG of Ar atoms in orthogonally-polarized laser fields. We also plotted the experimental single photoionization cross section [20] and our simulations based on the linear response theory [21]. In the simulations, we directly calculated the polarizability, with its real part relating to the refractive index of Ar gas, and the imaginary part representing the photoabsorption as shown in figure 5(a). Our simulations are in good agreement with the measurements for the photoionization as shown in figure 5(a) as well as for other atomic systems [22, 23].

Using our present model potential, the single photoionization cross section to the $d$-partial wave reaches zero or CM around 40 eV, which is lower than the measured one [20]. There is no CM for the $3p \rightarrow$ $s$-partial wave in that energy regime, and the cross section is much smaller. In the simulations, we chose the $z$-direction as the propagation direction of the IR pulses, and the $x$-direction as the direction of polarization. The polarization of the second harmonic laser field is along the $y$-direction.

To clearly show the physical origin of the CM, we also plot the HHG from Ar $3p_0$ (with magnetic quantum number $= 0$) in the single color laser field in figure 5(b). During the conservation of the magnetic quantum number, the $3p_0$ state can only reach a state with magnetic quantum number $m = \pm 1$, not an s-state by a photon polarized in the $x$-direction, therefore, $s$-partial wave does not contribute to the HHG and there is very deep minimum around harmonic order of 30. This shows that the present model potential can be used to investigate the CM qualitatively although it differs from the measured one in position. Without the second harmonic laser, the HHG shows a clear CM in the power spectra as shown in

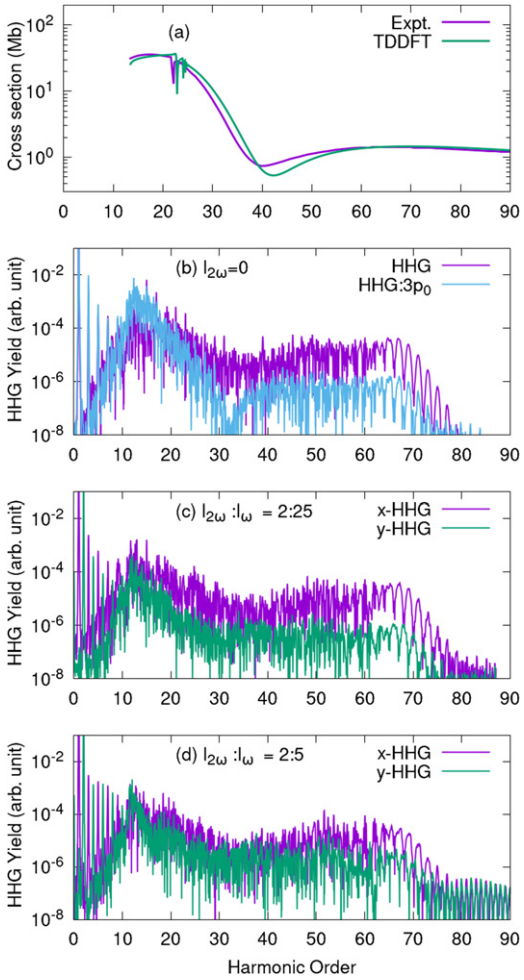


**Figure 5.** (a) Ar single photoionization cross sections from the experiment [20] and our simulations. Variation of HHG spectra generated from Ar atoms in two-color laser fields for (b) $I_\omega$:$I_{2\omega}$ = 1:0; (c) $I_\omega$:$I_{2\omega}$ = 25:2; and (d) $I_\omega$:$I_{2\omega}$ = 5:2 with $I_\omega = 2 \times 10^{14}$ W cm$^{-2}$.

figure 5(b) even after we sum all the contributions from $3p_{\pm1}$, $3p_0$ states coherently (the subscripts stand for the magnetic quantum numbers). The position is shifted and the width is broadened by the IR laser field due to the ac stark shift. The CM exists even in a very strong laser field. When a second harmonic laser field (polarized in the $y$-direction) orthogonal to the fundamental one (polarized in the $x$-direction) is added, both even and odd harmonics appear with even harmonics polarizing along the $y$-direction and odd harmonics polarizing along the $x$-direction as shown in figure 5(c). As the intensity of the second harmonics increases further, as shown in figure 5(d), the CM almost disappears. From the QRS theory [24], the time-dependent induced dipole is proportional to the transition dipole as well as the components of the given partial wave in the rescattering wave packet.

The CM or the zero of the transition matrix element from the ground state is determined by the differences of quantum defects between the initial and the final states [25–27], which is insensitive to the wavefunction or the external field in the outer region. The CM can be modified either by very strong external field, which modifies the behavior of wavefunction in the inner region, or by changing the trajectory of the rescattering electron to increase the non-CM partial wave contributions. Adding a second harmonic laser, the uni-directional rescattering electron is drifted off the lateral direction [28]. This modification of trajectory results in increasing the $s$-wave contribution and washing out the CM. If the intensity of the second harmonic increases further, the CM can be washed out completely, which is also consistent with the experimental results shown in figure 3(b). To see how the CM is washed out by the second laser field in atomic level, we show the HHG from $3p_0$ as a function of the intensity of the second laser field as shown in figure 6.

The CM around the HHG order of $3p_0$ is getting shadow when the second laser field is added, and finally disappears completely as the intensity increases further. Note that the measured HHG comes from all the sub orbitals of $3p$, and $3p_0$ is a minor contributor. We use it to illustrate the mechanism of the CM in

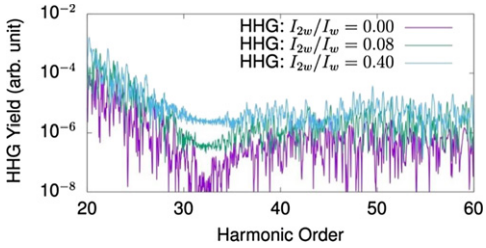


**Figure 6.** HHG of Ar $3p_0$ orbital as a function of the intensity of the second laser field. $I_\omega = 2 \times 10^{14}$ W cm$^{-2}$.

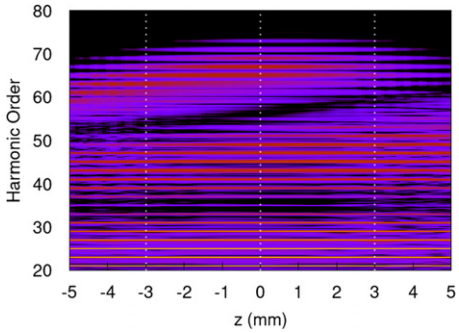


**Figure 7.** HHG of Ar atoms as a function of the gas jet position. The parameters used in the propagation are gas pressure of 70 Torr, jet diameter of 1 mm, and confocal parameter of 15 mm. The dashed lines mark the gas jet positions corresponding to the measurements in figure 4(a).

the two-color laser fields. We do not see clear sharp HHG peaks in figures 5 and 6 for atomic HHG. The measured HHG spectra are macroscopic spectra and propagation effects have to be considered.

The dipole corresponding to the measured one can be written as:

$$D(q) \propto \int \mathrm{d}_{\mathrm{atm}}(q, r, z)\, \mathrm{e}^{\mathrm{i}\Phi(q,r,z)}\, \mathrm{e}^{-\Gamma(q,z)} r \mathrm{d}r\mathrm{d}z, \tag{1}$$

Here, $d_{\mathrm{atm}}(q, r, z)$ is the atomic dipole of harmonic order $q$ emitted at space $(r, z)$, and $\Phi(q, r, z)$ is the propagation phase, which comes from differences of the geometry phase, atomic dispersion phase, and ionized electron plasma phase between the IR laser and the HHG. $\Gamma(q, z)$, self-absorption, can be expressed as:

$$\Gamma(q, z) = \int_z \sigma(q\omega)\, n(z)\, \mathrm{d}z, \tag{2}$$

with $\sigma(q\omega)$ being the photoabsorption cross section and $n(z)$ is the gas density at $z$ position. Unlike other theories that use the strong field approximation, we do not need atomic dipole phase from the long or short trajectories since this is taken into account automatically in our TDSE simulations. The detailed expressions of $\Phi(q, r, z)$ is given in reference [29]. We ignored the $r$-dependent geometric phase and only considered one-dimensional propagation. For atomic dispersion of HHG, we calculated the polarizability using the linear response theory [21]. Using the present experimental parameters, we calculated the macroscopic HHG. Figure 7 shows the HHG after the propagation as a function of the gas jet position. Here we assumed that the laser propagates along the $z$-axis as shown in figure 1. Although the IR intensity is symmetric about the focal plane, the HHG is not symmetric due to phase matching in the propagation. As shown in figure 4(a), the delayed maximum [27] after the CM in the HHG is broader at +3 mm, and is narrower at −3 mm, which is consistent with the simulations results in figure 7.

## 5. Summary

The disappearance of CM in the XUV harmonics spectra of Ar gas was observed in this work at different conditions of gas HHG experiments. The disappearance of the CM can be attributed to single atom responses in the microscopic domain as well as the phase matching conditions in the macroscopic domain. The CM at the microscopic level can be destroyed by adding a second orthogonal field, and the CM in the macroscopic can be tuned by the phase matching or changing the gas jet positions. Divergence of XUV

harmonics indicates a single active electron behavior in the electric field of femtosecond pulses due to the existence of both long and short trajectories [30]. Two-color HHG can minimize the divergence and improve the flux at the same time by tuning the relative phase of the two-color field to selectively enhance the short over the long trajectory emission. The width and depth of CM in XUV harmonics spectra in Ar gas was explored by changing beam aperture, the position of gas jet, and pumping by two orthogonally-polarized laser fields. We noted that the investigation nature of HHG in atoms or molecules, especially with CM, requires precise knowledge of the exact position of gas jet during the experimental studies.

The dynamics of Cooper-like minima near the cutoff of the HHG spectra from $N_2$ molecules were explored by Bertrand *et al* [31]. It was shown that the CM minimum in the transition moment along the molecular axis appears at about 45 eV, which is attributed to the transition moment going through a minimum due to destructive interference between dominant partial wave components. The dynamics of Cooper-like minima near the cutoff of the HHG spectra from $N_2$ molecules driven by intense femtosecond lasers at three different wavelengths (i.e., 1300, 1400 and 1500 nm) were explored by Li *et al* [32]. Variation in the CM position, from 80 eV to 102 eV, for $N_2$ molecules was observed by changing the intensity of the laser pulses. It was shown that the spectral depth position depends linearly on the peak intensity of the driving field. Since there are competing channels the laser intensity and/or phase matching can change both the position and pattern of CM in $N_2$ HHG spectra. In our case we did not reach HHG orders up to 93 eV spectral range for $N_2$ gas at the present laser energy and wavelength. The observed harmonic spectra for $N_2$ and $O_2$ were typical HHG spectra that can be described by Lewenstien three-step model based on the strong field approximation [33]. The spectra observed for these two molecules are typical ones with universal shape of HHG distribution, in which it falls for the first few order of harmonics, then exhibits a plateau where all harmonics have the same strength, and ends up with a sharp cutoff. The measured recombination dipole matrix phase agrees well with the predictions based on the scattering phases and amplitudes of the interfering s- and d-channel contributions to the complementary photoionization process [34].

## 6. Conclusion

In conclusion, we analyzed the variations of the Cooper minimum (CM) in the HHG spectra generated during the interaction of Ar gas with 1030 nm, 35 fs, 50 kHz laser pulses. The control of the depth and width of CM in argon gas was demonstrated by changing the jet position with respect to the focal plane of focusing lens and by defocusing-assisted phase matching. The dynamics of the odd and even harmonic yields were investigated by applying orthogonally-polarized fields of the fundamental radiation and its second harmonic. Our experimental findings are supported by theoretical calculations that solve the time-dependent Schrödinger equation in microscopic domain, and take into account the phase matching in the macroscopic domain.

## Funding

This work was supported by the American University of Sharjah through FRG AS1801 Grant and the AUS-Common Research Facility. XMT was supported by Grants-in-Aid for Scientific Research (JP16K05495) from the Japan Society for the Promotion of Science and the simulation was supported by Multidisciplinary Cooperative Research Program in CCS, University of Tsukuba.

## Acknowledgments

The work in this paper was supported, in part, by the Open Access Program from the American University of Sharjah. This paper represents the opinions of the authors and does not mean to represent the position or opinions of the American University of Sharjah.

## ORCID iDs

A S Alnaser https://orcid.org/0000-0003-4822-9747

## References

[1] Antoine A, L'Huillier A and Lewenstein M 1996 *Phys. Rev. Lett.* **77** 1234
[2] Leeuwenburgh J, Cooper B, Averbukh A, Marangos J P and Ivanov M 2013 *Phys. Rev. Lett.* **111** 123002

[3] Higuet J et al 2011 Phys. Rev. A 83 053401
[4] Shiner A D, Schmidt B E, Trallero-Herrero C, Corkum P B, Kieffer J-C Legare F and Villeneuve D M 2012 J. Phys. B: At. Mol. Opt. Phys. 45 074010
[5] Shiner A D, Schmidt B E, Trallero-Herrero C, Worner H J, Patchkovskii S, Corkum P M, Kieffer J-C Legare F and Villeneuve D M 2011 Nat. Phys. 7 464
[6] Cooper J W 1962 Phys. Rev. 128 681
[7] Wong M C H, Le A-T, Alharbi A F, Boguslavskiy A E, Lucchese R R, Brichta J-P, Lin C D and Bhardwaj V R 2013 Phys. Rev. Lett. 110 033006
[8] Corkum P B 1993 Phys. Rev. Lett. 71 1994
[9] Jin C 2013 Theory of Nonlinear Propagation of High Harmonics Generated in a Gaseous Medium (Berlin: Springer)
[10] Le A-T, Lucchese R R, Tonzani S, Morishita T and Lin C D 2009 Phys. Rev. A 80 013401
[11] Jin C and Lin C D 2012 Phys. Rev. A 85 033423
[12] Worner H J, Niikura H, Bertrand J B, Corkum P M and Villeneuve D M 2009 Phys. Rev. Lett. 102 103901
[13] Farrell J P, Spector L S, McFarland B K, Bucksbaum P H, Gühr M, Gaarde M B and Schafer K J 2011 Phys. Rev. A 83 023420
[14] Colosimo P et al 2008 Nat. Phys. 4 386
[15] Takahashi E J, Kanai T, Nabekawa Y and Midorikawa K 2008 Appl. Phys. Lett. 93 041111
[16] Ganeev R A, Singhal H, Naik P A, Kulagin I A, Redkin P V, Chakera J A, Tayyab M, Khan R A and Gupta P D 2009 Phys. Rev. A 80 033845
[17] Shan B, Tong X M, Zhao Z, Chang Z and Lin C D 2002 Phys. Rev. A 66 061401
[18] Tong X M and Lin C D 2005 J. Phys. B: At. Mol. Opt. Phys. 38 2593
[19] Gao X and Tong X M 2019 Phys. Rev. A 100 063424
[20] Samson J R and Stolte W C 2002 J. Electron Spectrosc. Relat. Phenom. 123 265
[21] Tong X M and Chu S I 1997 Phys. Rev. A 55 3406
[22] Domondon A T and Tong X M 2002 Phys. Rev. A 65 032718
[23] Watanabe T, Domondon A T and Tong X M 2009 Phys. Rev. A 80 042709
[24] Morishita T, Le A T, Chen Z and Lin C D 2008 Phys. Rev. Lett. 100 013903
[25] Msezane A Z and Manson S T 1982 Phys. Rev. Lett. 48 473
[26] Aymar M, Robaux O and Wane S 1984 J. Phys. B: At. Mol. Phys. 17 993
[27] Tong X-M, Li J M and Pratt R H 1990 Phys. Rev. A 42 5348
[28] Kim I J, Kim C M, Kim H T, Lee G H, Lee Y S, Park J Y, Cho D J and Nam C H 2005 Phys. Rev. Lett. 94 243901
[29] Pfeifer T, Spielmann C and Gerber G 2006 Rep. Prog. Phys. 69 443
[30] Roscam Abbing S, Campi F, Sajjadian F S, Lin N, Smorenburg P and Kraus P M 2019 arXiv:1910.06470
[31] Bertrand J B, Wörner H J, Hockett P, Villeneuve D M and Corkum P B 2012 Phys. Rev. Lett. 109 143001
[32] Li G et al 2013 arXiv:1306.0177v1
[33] Lewenstein M, Balcou P, Ivanov M, L'Huillier A and Corkum P B 1994 Phys. Rev. A 49 2117
[34] Schoun S B, Chirla R, Wheeler J, Roedig C, Agostini P and DiMauro L F 2014 Phys. Rev. Lett. 112 153001